

Distilling a Powerful Student Model via Online Knowledge Distillation

Shaojie Li¹, Mingbao Lin¹, Yan Wang³, Feiyue Huang⁴,
Yongjian Wu⁴, Yonghong Tian⁵, Ling Shao⁶, Rongrong Ji^{1,2*}

¹Media Analysis and Computing Lab, Department of Artificial Intelligence,
School of Informatics, Xiamen University, China

²Institute of Artificial Intelligence, Xiamen University, China

³Pinterest, USA ⁴Tencent Youtu Lab, China ⁵ Peking University, China

⁶Inception Institute of Artificial Intelligence, Abu Dhabi, UAE

Abstract

Existing online knowledge distillation approaches either adopt the student with the best performance or construct an ensemble model for better holistic performance. However, the former strategy ignores other students' information, while the latter increases the computational complexity. In this paper, we propose a novel method for online knowledge distillation, termed FFSD, which comprises two key components: Feature Fusion and Self-Distillation, towards solving the above problems in a unified framework. Different from previous works, where all students are treated equally, the proposed FFSD splits them into a student leader and a common student set. Then, the feature fusion module converts the concatenation of feature maps from all common students into a fused feature map. The fused representation is used to assist the learning of the student leader. To enable the student leader to absorb more diverse information, we design an enhancement strategy to increase the diversity among students. Besides, a self-distillation module is adopted to convert the feature map of deeper layers into a shallower one. Then, the shallower layers are encouraged to mimic the transformed feature maps of the deeper layers, which helps the students to generalize better. After training, we simply adopt the student leader, which achieves superior performance, over the common students, without increasing the storage or inference cost. Extensive experiments on CIFAR-100 and ImageNet demonstrate the superiority of our FFSD over existing works. The code is available at <https://github.com/SJLeo/FFSD>.

1. Introduction

Deep neural networks (DNNs) have achieved unprecedented success in various visual tasks, including image clas-

sification [9, 33], object detection [5, 28], and image generation [26, 46]. Nevertheless, their extensive memory and computational requirements severely hinder their deployment in resource-limited devices. To alleviate this problem, several techniques have been developed to derive a light-weight model with negligible compromise in performance. Examples include network pruning [8, 10], parameter quantization [27, 15], low-rank decomposition [3, 44] and knowledge distillation [12, 29].

Among them, knowledge distillation has received particular attention, transferring knowledge from a high-capacity teacher [12, 29, 40], or an online ensemble [45, 32, 47], to a student model. Traditional knowledge distillation methods use a two-stage optimization where a cumbersome teacher network has to be trained in advance in order to yield a high-capacity model, which then serves as supervision information to guide the training of a light-weight student network. Though progress has been made, these methods require significant training time due to their heavy dependence on a large-scale teacher model.

This has motivated the community to simplify the training procedure by exploring online knowledge distillation [45, 47], where a collection of student models are trained simultaneously in a collaborative manner without the involvement of a large-scale teacher model. Existing online knowledge distillation can be implemented by either mutual learning [45, 1, 2, 43] or ensemble learning [47, 32, 7, 17]. The former aligns the soft outputs of all students so as to allow message passing among them. Then, the student model with the optimal performance is adopted as the final model. However, the message passing does not guarantee that one single student will carry all the information of the ensemble. This limits the distillation performance. In contrast, the latter constructs a virtual teacher by ensembling the outputs of all the students, which are then distilled back to foster each student. Nevertheless, this group has to retain all the student models so as to en-

*Corresponding Author: rrji@xmu.edu.cn

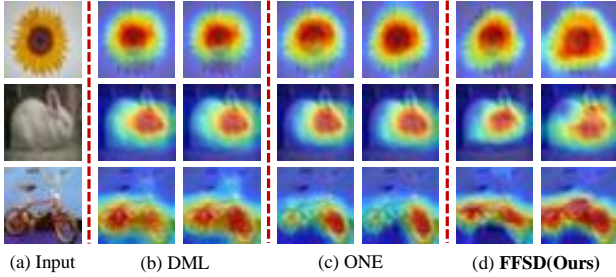


Figure 1. Feature map visualization of the two student models from online knowledge distillation methods including DML [45], ONE [47] and our proposed FFSD, using ResNet-32 on CIFAR-100. Feature maps from different student models are highly similar in DML [45] and ONE [47]. In contrast, the proposed FFSD can learn diversified feature maps for different student models.

semble their output logits together to pursue better performance, which significantly increases the memory consumption and computational complexity since all models have to be stored in disks and evaluated during inference. Thus, online knowledge distillation remains an open problem.

In this paper, we present a novel online knowledge distillation method, introducing two key modules, *i.e.*, feature fusion and self-distillation (FFSD), in order to solve the above problems in a unified framework. Specifically, we construct a common student set and a student leader, which share the same network architecture. The common student set is trained through mutual learning. In order to take full advantage of the rich information of all common students in the set, we design a feature fusion module similar to an autoencoder to fuse the output feature maps from all common students, and then distill it to the student leader. First, it encodes the common students’ output feature maps into a meaningful compact feature map with the same size as the student leader, and then the student leader is encouraged to mimic this fused feature map. Meanwhile, the output feature map of the student leader is decoded back to match the concatenated feature maps of all common students to ensure the effectiveness of the feature map learned by the student leader. However, as shown in Fig. 1, the activation feature maps of mutual learning and ensemble learning are highly overlapped, which means that the common students all pay more attention to exactly the same area of the input image. The student leader thus cannot obtain additional information from the fused feature map. To address this issue, we devise a strategy to enhance the feature diversity of the common student models in the set. Specifically, we construct a diverse feature map by shifting the focus of the output feature map of a student. The diverse feature map is further distilled to other students. In addition, we design a self-distillation module that converts high-order supervision information (the fused feature map and the diverse

feature map) to low-order supervision information for shallower network layers. Self-distillation facilitates the flow of supervision information from deeper to shallower network layers. It thus enriches the supervision information in the training process. After training, only the student leader is retained for deployment, as it achieves superior performance over all other students. We empirically demonstrate the effectiveness of our proposed FFSD method with extensive experiments on the CIFAR-100 [18] and ImageNet [30] datasets.

Our contributions are summarized as follows:

- A novel online knowledge distillation method, FFSD, is proposed to improve distillation performance. We design a feature fusion module equipped with a diversity enhancement strategy to integrate the knowledge of students and distill it to the student leader, which improves the generality of the final model.
- A self-distillation module is proposed to convert high-order supervision information to low-order cues for shallower network layers, which provides richer information for model training.
- Extensive experiments on two benchmarks demonstrate the effectiveness of our proposed FFSD.

2. Related Work

Traditional Knowledge Distillation. Traditional distillation works transfer knowledge from a cumbersome teacher model to a light-weight student model. As such, a large-scale model has to be trained in advance, based on which various knowledge definitions and transfer strategies are proposed to boost the performance of the student model. The pioneering work [12] performs knowledge representation of a teacher model using the softmax output layer, which converts the logit into a soft probability with a temperature parameter. Following this, a large number of works proposed new forms of knowledge, such as intermediate feature maps [29], attention maps [40], second-order statistics [38], contrastive features [34, 36], or structured knowledge [24, 21, 25]. Another group of methods focus on transfer strategies so as to enable the student model to inherit knowledge from the teacher model. An intuitive solution is to use the Kullback-Leibler divergence or ℓ_p -loss when the knowledge falls on the soft logit [12, 20] or intermediate representation [29, 40]. Beyond that, Wang *et al.* [35] utilized the adversarial training scheme in generative adversarial networks (GANs) [6] to transfer knowledge. Jang *et al.* [16] considered meta-learning to selectively transfer knowledge. In [22], a reinforcement learning based architecture-aware distillation was proposed to pass the structural knowledge to the student.

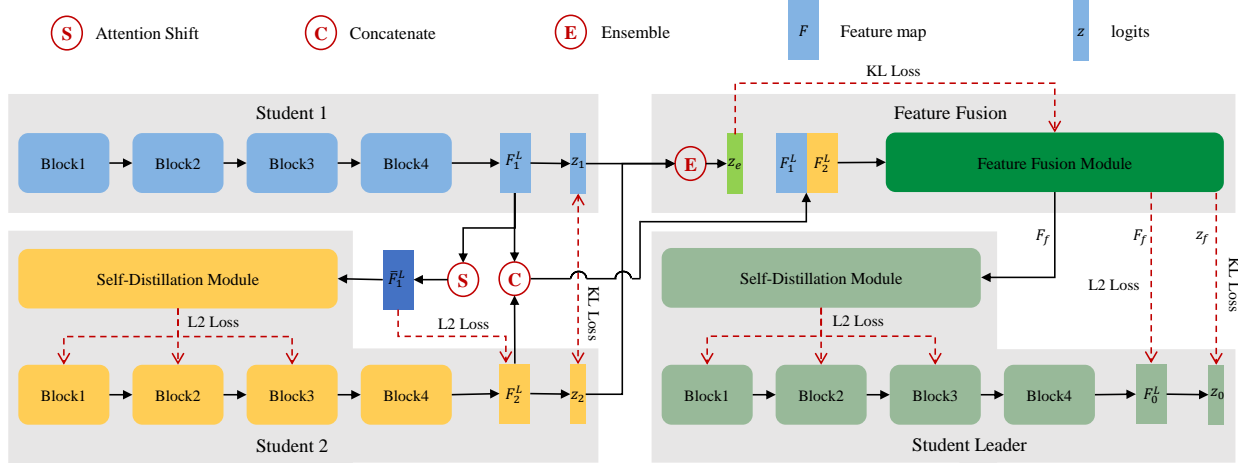


Figure 2. The framework of our proposed FFSD for online knowledge distillation. First, student 1 and student 2 learn from each other in a collaborative way. Then, by shifting the attention of student 1 and distilling it to student 2, we are able to enhance the diversity among students. Lastly, the feature fusion module fuses all the students’ information into a fused feature map. The fused representation is then used to assist the learning of the student leader. After training, we simply adopt the student leader, which achieves superior performance over all other students.

Online Knowledge Distillation. Online knowledge distillation has emerged as an alternative that eliminates the dependency on the cumbersome teacher model. It builds knowledge distillation based on a collection of student models that collaborate through simultaneous training. To this end, Zhang *et al.* [45] proposed a deep mutual learning strategy where pair-wise students are encouraged to learn from each other by a mimicry loss based on the Kullback-Leibler divergence. Chen *et al.* [1] performed two-level distillation by training multiple auxiliary peers and one group leader, separately. The former aims to boost peer diversity, while the latter transfers knowledge from an ensemble of auxiliary peers to the group leader. In [2], online knowledge distillation was built at a feature-map level using the adversarial training framework. Kim *et al.* [17] fused the intermediate representations of subnetworks, passing the result to an auxiliary classifier. Then, the knowledge from the auxiliary classifier is delivered back to each subnetwork for mutual teaching. In [47, 32, 7], all student branches are ensembled to construct a stronger teacher model, which is in turn distilled back to the students to enhance the model learning.

Self-Distillation. Self-distillation, originally proposed by Furlanello *et al.* [4], has received a great deal of attention recently, due to its distillation of knowledge within the network itself without the aid of other models. Augmentation based works [19, 37] focus on self-distillation via data augmentation of the input images. Hou *et al.* [13] and Zhang *et al.* [42] distilled deeper parts of the network as the conceptual teacher model to guide the learning of shallower modules. Li *et al.* [39] revisited knowledge distillation as a type of learned label smoothing regularization, and accord-

ingly proposed a novel teacher-free knowledge distillation framework where the student model learns from itself or a manually designed regularization distribution.

3. The Proposed Method

3.1. Preliminaries

Consider a group of $n + 1$ student models $\mathbf{G} = \{\mathbf{S}_i\}_{i=0}^n$, all of which share the same network structure and consist of L convolutional layers. For each model \mathbf{S}_i , we denote the output of the feature maps in the l -th layer as $\mathbf{F}_i^l \in \mathbb{R}^{C^l \times H^l \times W^l}$, where C^l, H^l, W^l denote the channel number, height and width of a feature map, respectively. Besides, given a labeled dataset $\mathcal{D} = \{(\mathbf{x}, \mathbf{y})\}$ with K classes, the logit produced by student \mathbf{S}_i is denoted as $\mathbf{z}_i \in \mathbb{R}^K$.

Then, the prediction probability of the softmax layer is represented by \mathbf{p}_i , with the probability for the k -th class computed as

$$\mathbf{p}_i^k = \frac{\exp(\mathbf{z}_i^k/T)}{\sum_{k=1}^K \exp(\mathbf{z}_i^k/T)}, \quad (1)$$

where $T \geq 1$ is the temperature parameter used to soften the output probability. When $T = 1$, it degenerates to the original softmax output. For ease of representation, we consider \mathbf{p}_i as having temperature $T = 1$; otherwise, we rewrite it as $\hat{\mathbf{p}}_i$.

Existing literature encourages all students $\mathbf{S}_i \in \mathbf{G}$ to learn from each other. Then, the resulting model for deployment falls on the optimal student or the ensemble one. As discussed in Sec. 1, the former ignores the efficacy of other

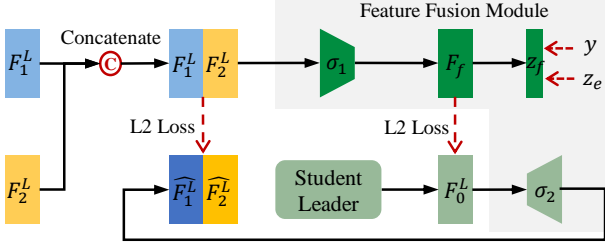


Figure 3. Feature fusion for the feature learning of the student leader. The whole learning scheme uses an autoencoder framework that forces the last-layer output feature map \mathbf{F}_0^L of the student leader to mimic the fused feature map \mathbf{F}_f .

students, while the latter increases the resource burden. Differently, in this paper, we innovatively propose to regard \mathbf{S}_0 as the student leader and the remaining $\hat{\mathbf{G}} = \mathbf{G} - \{\mathbf{S}_0\}$ as a common student set. Then, students in $\hat{\mathbf{G}}$ learn in a collaborative manner, while the student leader \mathbf{S}_0 is responsible for learning the knowledge from the common students. Note that all students mentioned below represent the common students in the set $\hat{\mathbf{G}}$ and not the student leader.

Following [45], we first define the training objective $\mathcal{L}_{\text{base}}$ for the collaborative learning of the students as

$$\mathcal{L}_{\text{base}} = \mathcal{L}_{CE}(\mathbf{y}, \mathbf{p}_i) + T^2 \sum_{j=1, j \neq i}^n \mathcal{L}_{KL}(\hat{\mathbf{p}}_j || \hat{\mathbf{p}}_i), \quad (2)$$

where \mathcal{L}_{CE} is the cross-entropy loss between the one-hot ground-truth label \mathbf{y} and the prediction \mathbf{p}_i . The \mathcal{L}_{KL} from $\hat{\mathbf{p}}_i$ to $\hat{\mathbf{p}}_j$ is computed as

$$\mathcal{L}_{KL}(\hat{\mathbf{p}}_j || \hat{\mathbf{p}}_i) = \sum_{k=1}^K \hat{\mathbf{p}}_j^k \log \frac{\hat{\mathbf{p}}_j^k}{\hat{\mathbf{p}}_i^k}. \quad (3)$$

We multiply the \mathcal{L}_{KL} with T^2 because the gradients produced by the soft predictions are scaled by $1/T^2$.

3.2. Feature Fusion

To maximize the usage of the students' information, we design a feature fusion module, the structure of which is displayed in Fig. 3, to fuse the feature maps of all students. The result is then distilled to strengthen the capacity of the student leader \mathbf{S}_0 .

Specifically, we first concatenate the feature maps in the L -th convolutional layers of all common students, *i.e.*, $\{\mathbf{F}_i^L\}_{i=1}^n$, the result of which is denoted as \mathbf{F}_e . The fusion module encodes the concatenated feature maps into a meaningful compact feature map \mathbf{F}_f with the same size as the student leader. This fused feature map is then passed into a fusion classifier supervised by the ground-truth labels and the ensemble logit of students $\mathbf{z}_e = \frac{1}{n} \sum_{i=1}^n \mathbf{z}_i$ [45, 32].

We further denote the output logit of the fusion classifier as \mathbf{z}_f . By transferring these logits into prediction probabilities using Eq. (1), the corresponding training objective for the fusion classifier is computed as follows:

$$\mathcal{L}_{\text{fusion}} = \mathcal{L}_{CE}(\mathbf{y}, \mathbf{p}_f) + T^2 \mathcal{L}_{KL}(\hat{\mathbf{p}}_e || \hat{\mathbf{p}}_f). \quad (4)$$

We aim to transfer the high-quality information from the fused feature map to the student leader. To this end, we encourage the last-layer output of the student leader \mathbf{F}_0^L to learn from the fused feature map. Meanwhile, the output feature map of the student leader is decoded back to match the concatenated feature maps of all the students to ensure the effectiveness of the feature map learned by the student leader. Hence, we can derive our optimization objective for the output feature map of the student leader as follows:

$$\mathcal{L}_{\mathbf{F}_0^L} = \left\| \frac{\mathbf{F}_0^L}{\|\mathbf{F}_0^L\|_2} - \frac{\mathbf{F}_f}{\|\mathbf{F}_f\|_2} \right\|_2 + \left\| \frac{\sigma(\mathbf{F}_0^L)}{\|\sigma(\mathbf{F}_0^L)\|_2} - \frac{\mathbf{F}_e}{\|\mathbf{F}_e\|_2} \right\|_2, \quad (5)$$

where $\|\cdot\|_2$ is the ℓ_2 -norm and $\sigma(\cdot)$ aligns the channel dimension of \mathbf{F}_0^L to \mathbf{F}_e .

Note that [31] also conducts layer-wise feature amalgamation from multiple teachers, but we only perform feature fusion in the last layer and distill the fused feature map to the shallower layers through our proposed self-distillation. During the feature fusion process, we set up an additional classifier to supervise the quality of the fused features, which is not available in [31]. In addition, as illustrated in Fig. 1, the output representations when using mutual learning [45] or ensemble learning [47] tend to be unified, which can prevent the student leader from obtaining additional information from the feature fusion. Therefore, it is necessary to diversify the outputs of students, which is totally ignored in [31]. A straightforward solution can be directly borrowed from [29, 23, 11], which essentially minimizes the negative reconstruction error on the intermediate outputs as

$$\mathcal{L}_{\text{div}} = -\frac{1}{L} \sum_{i=1, j=1, i \neq j}^n \sum_{l=1}^L \|\mathbf{F}_i^l - \mathbf{F}_j^l\|_2. \quad (6)$$

However, minimizing Eq. (6) raises some concerns: (1) **Significant computational complexity.** As can be seen from Eq. (6), a total of $n(n-1)L$ ℓ_2 -norm distances have to be computed. (2) **Task independence.** The goal of the ℓ_2 -norm loss is to reduce the overall error, which will shift the attention of feature maps to a task-independent position. (3) **Attention inconsistency.** The per-layer loss is calculated separately, ignoring the coherence of attentions across different layers of the network.

To reduce the diversity computation in Eq. (6), we propose to train the first student \mathbf{S}_1 using Eq. (2), where student $\mathbf{S}_i (i > 1)$ only performs diversity enhancement calculation

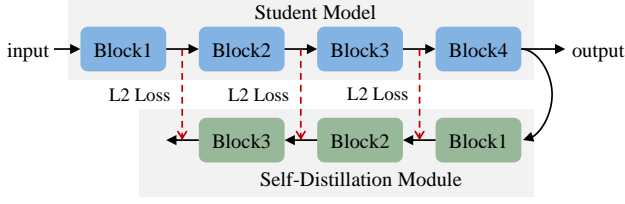


Figure 4. Training scheme of the self-distillation module.

with student \mathbf{S}_{i-1} . Thus, our diversity enhancement learning transfers each student’s knowledge to the next peer student in a one-way chain manner. Nevertheless, diversifying feature maps from all layers still incurs high complexity. Instead, we empirically observe that using a small portion can perform well. To this end, we choose layers just before a downscaling operation, *e.g.* the last layer of each residual block for ResNet [9]. We denote the selected feature maps of student \mathbf{S}_i as $\{\mathbf{F}_i^m\}_{m=1}^M \in \{\mathbf{F}_i^l\}_{l=1}^L$ for diversity. It is worth noting that $\mathbf{F}_i^M = \mathbf{F}_i^L$.

The diversity is essentially enhanced to enable the attention of students to concentrate on different image positions. Following this, we first extract the attention for each feature map \mathbf{F}_i^m using the scheme in [40], as

$$\mathbf{A}_i^m = \sum_{c=1}^{C^m} |\mathbf{F}_i^m(c, :, :)|^2. \quad (7)$$

Then, the diversity enhancement attention map $\bar{\mathbf{A}}_i^m$ is computed as

$$\bar{\mathbf{A}}_i^m = \left(\frac{P}{2} - \mathbf{A}_i^m\right) \times \text{sign}(\mathbf{A}_i^m - t) + \frac{P}{2}, \quad (8)$$

where $P = \|\mathbf{A}_i^m\|_2$ and t is a threshold, empirically set as the $\frac{H^m \times W^m}{3}$ -th smallest number in \mathbf{A}_i^m . The goal of Eq. (8) is to shift attention \mathbf{A}_i^m to the slightly weaker areas, while maintaining the attention value of task-independent areas by setting threshold t . After that, we derive our diversity enhancement objective for \mathbf{S}_i ($i > 1$) to replace Eq. (6) as

$$\mathcal{L}_{\text{div}} = \sum_{m=1}^M \left\| \frac{\mathbf{A}_i^m}{\|\mathbf{A}_i^m\|_2} - \frac{\bar{\mathbf{A}}_{i-1}^m}{\|\bar{\mathbf{A}}_{i-1}^m\|_2} \right\|_2. \quad (9)$$

Though we achieve diversity between student \mathbf{S}_i and \mathbf{S}_{i-1} , the third concern, *i.e.*, the attention inconsistency, remains unsolved, which is our focus in Sec. 3.3.

3.3. Self-Distillation

In this section, we design a novel self-distillation module to convert high-order information to low-order information for shallower layers. The self-distillation module consists of $M - 1$ blocks, each of which learns to map \mathbf{F}_i^{m+1} back to \mathbf{F}_i^m . Specifically, each block is stacked with

Algorithm 1 Online knowledge distillation using Feature Fusion and Self-Distillation (FFSD)

Require: A common student set $\{\mathbf{S}_i\}_{i=1}^n$, a student leader \mathbf{S}_0 , a feature fusion module \mathbf{FF} and self-distillation modules $\{\mathbf{SD}\}_{i=0}^n$.

Ensure: A powerful student leader \mathbf{S}_0 .

- 1: **for** iter = 1 : Iter **do**
 - 2: **for** i = 1 : n **do**
 - 3: Forward the common student \mathbf{S}_i and compute intermediate feature maps $\{\mathbf{F}_i^m\}_{m=1}^M$.
 - 4: **end for**
 - 5: Forward the student leader \mathbf{S}_0 .
 - 6: Forward the feature fusion module \mathbf{FF} using the feature map \mathbf{F}_e concatenated by $\{\mathbf{F}_i^M\}_{i=1}^n$.
 - 7: Update the common student \mathbf{S}_1 using Eq. (2).
 - 8: **for** i = 2 : n **do**
 - 9: Update the common student \mathbf{S}_i using Eq. (12).
 - 10: **end for**
 - 11: Update the student leader \mathbf{S}_0 using Eq. (13).
 - 12: Update the feature fusion module \mathbf{FF} using Eq. (4).
 - 13: **for** i = 0 : n **do**
 - 14: Update the self-distillation module \mathbf{SD}_i using Eq. (10).
 - 15: **end for**
 - 16: **end for**
-

a transpose convolutional layer, batch normalization layer and ReLU layer. We denote the feature maps of each block as $\{\mathbf{F}_i^m\}_{m=1}^{M-1}$ in a top-down order and their corresponding attention maps $\{\mathbf{A}_i^m\}_{m=1}^{M-1}$ are calculated by Eq. (7). We equip each student with a self-distillation module, since each student has its own feature mapping. We train the self-distillation module together with the students, and in turn use it to distill the fused/diversity-enhanced feature map to the corresponding student model.

Training of Self-Distillation Module. As shown in Fig. 4, the self-distillation module takes the feature maps $\{\mathbf{F}_i^m\}_{m=1}^M$ as the training datasets, in which the feature map \mathbf{F}_i^M of the last-layer output serves as the input of the module, and the feature maps $\{\mathbf{F}_i^m\}_{m=1}^{M-1}$ serve as the target of each block in the module. For student \mathbf{S}_i , the training objective of its self-distillation module is as follows:

$$\mathcal{L}_{\text{sdm}} = \sum_{m=1}^{M-1} \left\| \frac{\mathbf{A}_i^m}{\|\mathbf{A}_i^m\|_2} - \frac{\mathbf{A}_i^m}{\|\mathbf{A}_i^m\|_2} \right\|_2 + \alpha \sum_{m=1}^{M-1} \left\| \frac{\mathbf{F}_i^m}{\|\mathbf{F}_i^m\|_2} - \frac{\mathbf{F}_i^m}{\|\mathbf{F}_i^m\|_2} \right\|_2, \quad (10)$$

where α balances the two loss terms. Due to the limited learning ability of the self-distillation module, we prefer to use it to learn the simple mapping of attention maps. Though an individual self-distillation block cannot completely map \mathbf{F}_i^{m+1} back to \mathbf{F}_i^m , we still encourage its output \mathbf{F}_i^m to be close to \mathbf{F}_i^m .

Application of Self-Distillation Module. Thanks to the

| Model | Baseline (%) | 2Net Avg (%) | Ens (%) | Fusion (%) | Leader (%) | Gain(↑) |
|----------------|--------------|--------------|--------------|--------------|--------------|-------------|
| ResNet-20 | 68.58 ± 0.26 | 71.92 ± 0.19 | 77.44 ± 0.14 | 73.43 ± 0.13 | 72.70 ± 0.13 | 4.12 ± 0.35 |
| ResNet-32 | 69.96 ± 0.30 | 74.25 ± 0.08 | 79.93 ± 0.11 | 76.04 ± 0.17 | 74.85 ± 0.05 | 4.90 ± 0.25 |
| ResNet-56 | 71.55 ± 0.50 | 75.61 ± 0.32 | 81.51 ± 0.16 | 77.28 ± 0.26 | 75.80 ± 0.11 | 4.25 ± 0.48 |
| WRN-16-2 | 71.97 ± 0.09 | 75.41 ± 0.21 | 80.26 ± 0.25 | 76.69 ± 0.11 | 75.81 ± 0.08 | 3.83 ± 0.03 |
| WRN-40-2 | 75.58 ± 0.17 | 78.73 ± 0.22 | 83.95 ± 0.26 | 80.24 ± 0.29 | 79.14 ± 0.03 | 3.47 ± 0.07 |
| GoogLeNet | 78.28 ± 0.24 | 81.48 ± 0.10 | 85.28 ± 0.13 | 82.42 ± 0.08 | 81.60 ± 0.25 | 3.32 ± 0.43 |
| DenseNet-40-12 | 73.70 ± 0.10 | 76.87 ± 0.14 | 81.60 ± 0.12 | 78.34 ± 0.14 | 77.39 ± 0.23 | 3.68 ± 0.33 |

Table 1. Experimental results on CIFAR-100. The ‘Baseline’ trains the model using ground-truth labels only, ‘2Net Avg’ represents the average accuracy of the two common students, and ‘Ens’ represents the accuracy of the correct prediction of either student network. ‘Fusion’ and ‘Leader’ represent the accuracy of the fusion classifier and the student leader, respectively. All results reported are computed as the median (standard deviations) of three runs.

good feature mapping ability of the self-distillation module, we can distill the last layer of the diversity enhancement objective to the shallower layers through the self-distillation module. This achieves the diversity enhancement of the whole network, while ensuring the attention consistency and task dependence mentioned in Section 3.2. In addition, we can still use the self-distillation module to distill the fused feature map to guide the training of shallower layers of the student leader.

For diversity enhancement, we first transform the diversity attention objective $\bar{\mathbf{A}}_{i-1}^M$ back into the diversity feature objective $\bar{\mathbf{F}}_{i-1}^M$ as the input of the self-distillation module. Then, the self-distillation module outputs the diversity objective $\{\bar{\mathbf{A}}_{i-1}^m\}_{m=1}^{M-1}$ of the shallower layers. The diversity enhancement objective of student $\mathbf{S}_i (i > 1)$ thus becomes

$$\mathcal{L}_{\text{div}} = \sum_{m=1}^{M-1} \left\| \frac{\mathbf{A}_i^m}{\|\mathbf{A}_i^m\|_2} - \frac{\bar{\mathbf{A}}_{i-1}^m}{\|\bar{\mathbf{A}}_{i-1}^m\|_2} \right\|_2 + \left\| \frac{\mathbf{A}_i^M}{\|\mathbf{A}_i^M\|_2} - \frac{\bar{\mathbf{A}}_{i-1}^M}{\|\bar{\mathbf{A}}_{i-1}^M\|_2} \right\|_2. \quad (11)$$

The final objective of the common students is as follows:

$$\mathcal{L}_{\text{stu}} = \mathcal{L}_{\text{base}} + \lambda_{\text{div}} \mathcal{L}_{\text{div}}, \quad (12)$$

where λ_{div} controls the importance of each term.

Similarly, we use our proposed self-distillation module to distill the fused feature map to shallower layers of the student leader. Therefore, the final objective of the student leader is as follows:

$$\mathcal{L}_{\mathbf{S}_0} = \mathcal{L}_{\text{CE}} + T^2 \mathcal{L}_{\text{KL}} + \lambda_{\text{fea}} \mathcal{L}_{\mathbf{F}_0^L} + \lambda_{\text{self}} \mathcal{L}_{\text{self}}, \quad (13)$$

where λ_{fea} and λ_{self} control the importance of each term.

The overall framework of our proposed FFSD is illustrated in Fig. 2. The training process can refer to Alg. 1.

4. Experiments

4.1. Experimental Settings

Datasets and Architecture. To evaluate the efficacy of our proposed FFSD online knowledge distillation method, we conduct experiments on two widely used datasets,

CIFAR-100 [18] and ImageNet [30]. CIFAR-100 contains 50k images with 100 object classes for training and 10k images for testing. ImageNet is a large-scale dataset containing 1.28M training images and 50k validation images of 1000 object classes. The size of each image is 32×32 for CIFAR-100 and 224×224 for ImageNet. To verify the generalization of our proposed method on different network architectures, we conduct experiments using ResNet [9], WRN [41], GoogLeNet [33], DenseNet [14].

Implementation Details. We use stochastic gradient descent (SGD) with Nesterov momentum to optimize the training objective. The initial learning rate, momentum and weight decay are set to 0.1, 0.9 and $1e-4$, respectively. For CIFAR-100, the models are trained with a batch size of 128 over 300 epochs and the learning rate is divided by 10 after 150 and 225 epochs. For ImageNet, we train all student models over 90 epochs with a batch size of 256. The learning rate warms up to 0.8 linearly in five epochs and is divided by 10 after 30 and 60 epochs. The feature fusion module uses the same implementation details described above. The self-distillation module is optimized by the ADAM optimizer with an initial learning rate of 0.001, using the same batch size, weight decay and learning rate decay strategy as the student model. The number of common students and temperature T are both set to 2.

4.2. Experimental Results

Results on CIFAR-100. We evaluate the effectiveness of FFSD on CIFAR-100 using seven popular networks, ResNet-20, ResNet-32, ResNet-56, WRN-16-2, WRN-40-2, GoogLeNet and DenseNet40-12. The experimental results are shown in Tab. 1. After feature fusion, the fusion classifier improves the accuracy over the baseline and students. This demonstrates that fusing the information of all students is of great help to the final result, and it is inappropriate to only adopt the optimal student as done in other methods. However, such performance improvements require retention of all students, which increases the storage and inference cost. Therefore, we distill the knowledge

| Method | ResNet-32 (%) | Gain(↑) | WRN-16-2 (%) | Gain(↑) |
|-------------------|---------------|-------------|--------------|-------------|
| Baseline | 69.96 | - | 71.97 | - |
| KD [12] | 72.87 | 2.91 | 73.79 | 1.82 |
| AT [40] | 71.23 | 1.27 | 73.70 | 1.73 |
| DML [45] | 73.64 | 3.68 | 74.63 | 2.66 |
| OKDDip [1] | 74.60 | 4.64 | 75.31 | 3.34 |
| AFD [2] | 74.03 | 4.07 | 75.33 | 3.36 |
| AMLN [43] | 74.69 | 4.73 | 75.56 | 3.59 |
| ONE [47] | 73.39 | 3.43 | 74.84 | 2.87 |
| FFL [17] | 74.44 | 4.48 | 75.26 | 3.29 |
| KDCL [7] | 74.30 | 4.34 | 75.50 | 3.53 |
| FFSD(Ours) | 74.85 | 4.90 | 75.81 | 3.84 |

Table 2. Results of our proposed FFSD compared with several state-of-the-art methods on CIFAR-100. In KT and AT, we use the pre-trained ResNet-56 and WRN-40-2 as the teacher model of ResNet-32 and WRN-16-2, respectively.

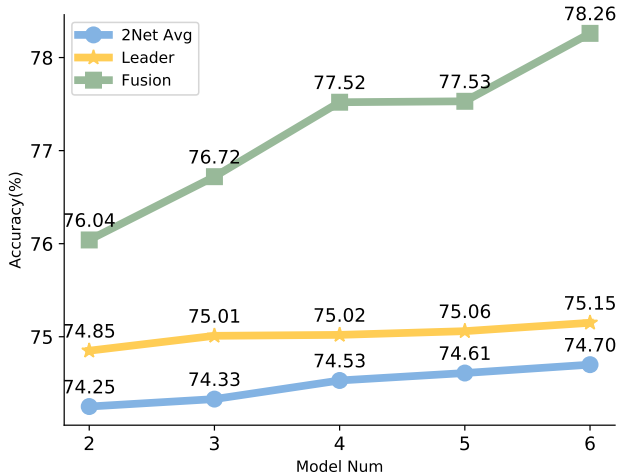


Figure 5. Experimental results when increasing the number of students using ResNet-32 on CIFAR-100.

from the feature fusion module to the student leader, which yields a 3.32%-4.90% improvement in accuracy over the baseline. Among the models compared, FFSD achieves a 4.90% performance improvement on ResNet-32 and 3.83% on WRN-16-2, results of which are superior to all other common students.

Quantitative Comparison on CIFAR-100. As shown in Tab. 2, we compare FFSD with several state-of-the-art methods on ResNet-32 and WRN-16-2. FFSD surpasses most knowledge distillation methods, including traditional knowledge distillation KD [12] and AT [40], mutual learning based DML [45], OKDDip [1], AFD [2] and AMLN [43], and ensemble learning based ONE [47], FFL [17] and KDCL [7]. For example, with ResNet-32, FFSD achieves an accuracy of 74.85%, which is higher than

| Model | Method | Top1-Acc (%) | Gain(↑) |
|-----------|-------------------|--------------|------------|
| ResNet-18 | Baseline | 69.7 | - |
| | DML [45] | 69.8 | 0.1 |
| | ONE [47] | 70.2 | 0.5 |
| | FFSD(Ours) | 70.9 | 1.2 |
| ResNet-34 | Baseline | 73.2 | - |
| | DML [45] | 74.0 | 0.8 |
| | ONE [47] | 74.1 | 0.9 |
| | FFSD(Ours) | 74.7 | 1.5 |

Table 3. Results of our proposed FFSD compared with several on-line knowledge distillation methods on ImageNet.

AMLN’s 74.69%. In addition, with WRN-16-2, FFSD can achieve a 3.84% performance improvement, which is superior to AMLN’s 3.59% and KDCL’s 3.53%. Not surprisingly, our proposed FFSD method has achieved the state-of-the-art results.

Results on ImageNet. We also conduct experiments on the large-scale and complex ImageNet dataset. We choose two most popular models, ResNet-18 and ResNet-34, for verification. As shown in Tab. 3, with ResNet-18, FFSD achieves 70.9% top-1 accuracy, which is superior to that of DML and ONE. For ResNet-34, FFSD can obtain a 1.5% accuracy boost, outperforming the baseline model and other online distillation methods. Hence, FFSD can effectively generalize to complex datasets.

Impact of Student Number. We increase the number of common students in group \mathcal{G} . The results are shown in Fig. 5. The accuracy of the students, the student leader, and the fusion classifier increase as the number of students grows. In fact, the fusion classifier achieves an astonishing accuracy of 78.26% after fusing the output feature maps of six students. The strategy of keeping only the optimal student after online knowledge distillation wastes the effective knowledge of other students. An interesting observation is that the accuracy of the student leader is always higher than the average accuracy of students, even when the number of students is up to six.

4.3. Detailed Analysis

Necessity of the Diversity Enhancement Strategy. We examine the effect of enhancing the diversity among students in the fusion classifier. As shown in Tab. 4, with ResNet-32, the cosine similarity of the two students in DML reaches 0.2635 without any diversity enhancement, and the fusion classifier can only achieve a 1.51% improvement in accuracy. Although the L2 method reduces the cosine similarity between the two students, minimizing Eq. (6) greatly affects the performance of the students. The goal of the ℓ_2 -norm loss is to minimize the overall average outputs, which lacks a clear objective. Our proposed FFSD presents a clear diversity enhancement strategy for attention shifting, which decreases the cosine similarity between the two students

| Model | DML [45] | | | L2 | | | FFSD | | |
|-----------|----------|--------|--------|----------|--------|--------|----------|--------|--------|
| | 2Net Avg | Fusion | Cosine | 2Net Avg | Fusion | Cosine | 2Net Avg | Fusion | Cosine |
| ResNet-32 | 73.64% | 75.15% | 0.2635 | 73.19% | 75.03% | 0.2351 | 74.25% | 76.04% | 0.2550 |
| WRN-16-2 | 74.63% | 76.18% | 0.2787 | 74.69% | 75.99% | 0.2570 | 75.41% | 76.69% | 0.2491 |

Table 4. Comparison between different diversity enhancement strategies. DML does not adopt any diversity enhancement strategy. L2 uses Eq. (6) for diversity enhancement. FFSD is our proposed diversity enhancement strategy. ‘Cosine’ represents the cosine similarity between the two student models.

| Model | L2 | | | L2 with SD | | | FFSD w/o SD | | | FFSD | | |
|----------|----------|--------|--------|------------|--------|--------|-------------|--------|--------|----------|--------|--------|
| | 2Net Avg | Fusion | Leader | 2Net Avg | Fusion | Leader | 2Net Avg | Fusion | Leader | 2Net Avg | Fusion | Leader |
| ResNet32 | 73.19% | 75.03% | 73.78% | 73.75% | 75.48% | 74.27% | 73.69% | 75.61% | 73.94% | 74.25% | 76.04% | 74.85% |
| WRN-16-2 | 74.69% | 75.99% | 75.20% | 75.00% | 76.15% | 75.33% | 74.63% | 76.05% | 75.43% | 75.41% | 76.69% | 75.81% |

Table 5. The effect of the self-distillation module on CIFAR-100. L2 uses Eq. (6) for diversity enhancement, which causes attention inconsistency. ‘SD’ represents our proposed self-distillation module.

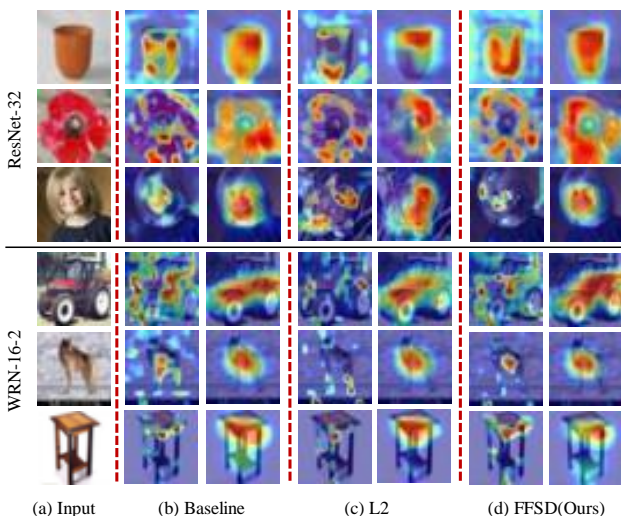


Figure 6. Feature map visualization with and without self-distillation on ResNet-32 and WRN-16-2. We use red dotted lines to separate the different methods. For each method, the left and right parts show the mid-, top-level activation feature maps, respectively. Among them, (a) are visual results of conventional training models, (b) uses Eq. (6) for diversity enhancement without self-distillation, and (c) is our proposed FFSD method with self-distillation.

and improves the performance of the models. Similar results are also observed on WRN-16-2, while the L2 method slightly improves the performance of the two students, the performance of the fusion classifier declines. Experimental results show that the proposed diversity enhancement strategy can effectively improve the performance of the fusion classifier.

Importance of the Self-Distillation. In Fig. 6, we visualize the difference between the activation feature maps with and without self-distillation. As can be seen from the baseline column, there is a significant overlap of attention positions between the activation feature maps of the mid-

| Model | DML [45]+SL | | ONE [47]+SL | |
|-----------|-------------|--------|-------------|--------|
| | Original | Leader | Original | Leader |
| ResNet-32 | 73.64% | 74.02% | 73.39% | 73.98% |
| WRN-16-2 | 74.63% | 75.15% | 74.84% | 75.44% |

Table 6. Experimental results of other online distillation methods combined with the student leader strategy on CIFAR-100. ‘SL’ represents the student leader.

and top-level, which illustrates the attention consistency within the network. However, it is difficult for us to see this phenomenon with the L2 method. The activation feature maps of the mid- and top-level only overlap in a very small part. Note that, in the picture of the wolf in row 5 of the L2 method, there is no way to find the attention consistency phenomenon, which is one of the reasons for the poor performance of the L2 method. Even though FFSD also enhances diversity, our proposed self-distillation addresses the problem of attention inconsistency.

Tab. 5 demonstrates the effect of self-distillation on the performance of the student models. We only retain the last-layer diversity enhancement loss calculation of the L2 method to enhance diversity and add self-distillation to it. All indicators are improved. We also investigate the effect of removing the self-distillation from FFSD. There is no doubt that the performance of students degrades, but it is still better than that with the L2 method. In conclusion, the introduction of self-distillation not only solves the problem of attention inconsistency during diversity enhancement, but also improves the performance of the student models.

The Advancement of the Student Leader. We combine the learning strategy of the student leader in FFSD with other online knowledge distillation methods for further experiments. From Tab. 6, we can see that the addition of the student leader injects vitality into other online knowledge distillation methods, and the performance of the student leader is improved. Among them, the combination of DML and the student leader yields a 0.38%-0.52% im-

provement in accuracy over the original results. The student leader also improves the performance of ONE by 0.59%-0.60%. The experimental results show the necessity of the student leader and the effectiveness of its learning strategy.

5. Conclusion

In this paper, a novel online knowledge distillation method, termed FFSD, is proposed using feature fusion and self-distillation. Existing online knowledge distillation methods either adopt the student with the best performance or consider the holistic performance using an ensemble model. However, they either ignore other students' information or increase the computational burden during deployment. To solve these issues, we first design a feature fusion module similar to an autoencoder to fuse the output feature maps from all students into a meaningful and compact fused feature map, which is then distilled to the student leader. At the same time, we design a diversity enhancement strategy to enhance the diversity among students, enabling the student leader to obtain more information during feature fusion. Second, a self-distillation module is proposed to convert the feature maps of deeper layers to shallower ones, which are then distilled to shallower layers. This increases the generalization ability of the model. Extensive experiments on CIFAR-100 and ImageNet demonstrate the superiority of our proposed FFSD.

6. Acknowledge

This work is supported by the National Science Fund for Distinguished Young Scholars (No.62025603), the National Natural Science Foundation of China (No.U1705262, No.62072386, No.62072387, No.62072389, No.62002305, No.61772443, No.61802324 and No.61702136) and Guangdong Basic and Applied Basic Research Foundation (No.2019B1515120049).

References

- [1] Defang Chen, Jian-Ping Mei, Can Wang, Yan Feng, and Chun Chen. Online knowledge distillation with diverse peers. In *Proceedings of the AAAI Conference on Artificial Intelligence (AAAI)*, pages 3430–3437, 2020. 1, 3, 7
- [2] Inseop Chung, SeongUk Park, Jangho Kim, and Nojun Kwak. Feature-map-level online adversarial knowledge distillation. *arXiv preprint arXiv:2002.01775*, 2020. 1, 3, 7
- [3] Emily L Denton, Wojciech Zaremba, Joan Bruna, Yann LeCun, and Rob Fergus. Exploiting linear structure within convolutional networks for efficient evaluation. In *Proceedings of the Advances in Neural Information Processing Systems (NeurIPS)*, pages 1269–1277, 2014. 1
- [4] Tommaso Furlanello, Zachary C Lipton, Michael Tschanen, Laurent Itti, and Anima Anandkumar. Born again neural networks. *arXiv preprint arXiv:1805.04770*, 2018. 3
- [5] Ross Girshick, Jeff Donahue, Trevor Darrell, and Jitendra Malik. Rich feature hierarchies for accurate object detection and semantic segmentation. In *Proceedings of the IEEE Conference on Computer Vision and Pattern Recognition (CVPR)*, pages 580–587, 2014. 1
- [6] Ian Goodfellow, Jean Pouget-Abadie, Mehdi Mirza, Bing Xu, David Warde-Farley, Sherjil Ozair, Aaron Courville, and Yoshua Bengio. Generative adversarial nets. In *Proceedings of the Advances in Neural Information Processing Systems (NeurIPS)*, pages 2672–2680, 2014. 2
- [7] Qiushan Guo, Xinjiang Wang, Yichao Wu, Zhipeng Yu, Ding Liang, Xiaolin Hu, and Ping Luo. Online knowledge distillation via collaborative learning. In *Proceedings of the IEEE Conference on Computer Vision and Pattern Recognition (CVPR)*, pages 11020–11029, 2020. 1, 3, 7
- [8] Song Han, Jeff Pool, John Tran, and William Dally. Learning both weights and connections for efficient neural network. In *Proceedings of the Advances in Neural Information Processing Systems (NeurIPS)*, pages 1135–1143, 2015. 1
- [9] Kaiming He, Xiangyu Zhang, Shaoqing Ren, and Jian Sun. Deep residual learning for image recognition. In *Proceedings of the IEEE Conference on Computer Vision and Pattern Recognition (CVPR)*, pages 770–778, 2016. 1, 5, 6
- [10] Yang He, Ping Liu, Ziwei Wang, Zhilan Hu, and Yi Yang. Filter pruning via geometric median for deep convolutional neural networks acceleration. In *Proceedings of the IEEE Conference on Computer Vision and Pattern Recognition (CVPR)*, pages 4340–4349, 2019. 1
- [11] Yihui He, Xiangyu Zhang, and Jian Sun. Channel pruning for accelerating very deep neural networks. In *Proceedings of the IEEE International Conference on Computer Vision (ICCV)*, pages 1389–1397, 2017. 4
- [12] Geoffrey Hinton, Oriol Vinyals, and Jeff Dean. Distilling the knowledge in a neural network. *arXiv preprint arXiv:1503.02531*, 2015. 1, 2, 7
- [13] Saihui Hou, Xinyu Pan, Chen Change Loy, Zilei Wang, and Dahua Lin. Learning a unified classifier incrementally via re-balancing. In *Proceedings of the IEEE Conference on Computer Vision and Pattern Recognition (CVPR)*, pages 831–839, 2019. 3
- [14] Gao Huang, Zhuang Liu, Laurens Van Der Maaten, and Kilian Q Weinberger. Densely connected convolutional networks. In *Proceedings of the IEEE Conference on Computer Vision and Pattern Recognition (CVPR)*, pages 4700–4708, 2017. 6
- [15] Benoit Jacob, Skirmantas Kligys, Bo Chen, Menglong Zhu, Matthew Tang, Andrew Howard, Hartwig Adam, and Dmitry Kalenichenko. Quantization and training of neural networks for efficient integer-arithmetic-only inference. In *Proceedings of the IEEE Conference on Computer Vision and Pattern Recognition (CVPR)*, pages 2704–2713, 2018. 1
- [16] Yunhun Jang, Hankook Lee, Sung Ju Hwang, and Jinwoo Shin. Learning what and where to transfer. *arXiv preprint arXiv:1905.05901*, 2019. 2
- [17] Jangho Kim, Minsung Hyun, Inseop Chung, and Nojun Kwak. Feature fusion for online mutual knowledge distillation. *arXiv preprint arXiv:1904.09058*, 2019. 1, 3, 7

- [18] Alex Krizhevsky, Geoffrey Hinton, et al. Learning multiple layers of features from tiny images. 2009. **2, 6**
- [19] Hankook Lee, Sung Ju Hwang, and Jinwoo Shin. Rethinking data augmentation: Self-supervision and self-distillation. *arXiv preprint arXiv:1910.05872*, 2019. **3**
- [20] Yuncheng Li, Jianchao Yang, Yale Song, Liangliang Cao, Jiebo Luo, and Li-Jia Li. Learning from noisy labels with distillation. In *Proceedings of the IEEE International Conference on Computer Vision (ICCV)*, pages 1910–1918, 2017. **2**
- [21] Yufan Liu, Jiajiong Cao, Bing Li, Chunfeng Yuan, Weiming Hu, Yangxi Li, and Yunqiang Duan. Knowledge distillation via instance relationship graph. In *Proceedings of the IEEE Conference on Computer Vision and Pattern Recognition (CVPR)*, pages 7096–7104, 2019. **2**
- [22] Yu Liu, Xuhui Jia, Mingxing Tan, Raviteja Vemulapalli, Yukun Zhu, Bradley Green, and Xiaogang Wang. Search to distill: Pearls are everywhere but not the eyes. In *Proceedings of the IEEE Conference on Computer Vision and Pattern Recognition (CVPR)*, pages 7539–7548, 2020. **2**
- [23] Jian-Hao Luo, Jianxin Wu, and Weiyao Lin. Thinet: A filter level pruning method for deep neural network compression. In *Proceedings of the IEEE International Conference on Computer Vision (ICCV)*, pages 5058–5066, 2017. **4**
- [24] Wonpyo Park, Dongju Kim, Yan Lu, and Minsu Cho. Relational knowledge distillation. In *Proceedings of the IEEE Conference on Computer Vision and Pattern Recognition (CVPR)*, pages 3967–3976, 2019. **2**
- [25] Nikolaos Passalis, Maria Tzelepi, and Anastasios Tefas. Heterogeneous knowledge distillation using information flow modeling. In *Proceedings of the IEEE Conference on Computer Vision and Pattern Recognition (CVPR)*, pages 2339–2348, 2020. **2**
- [26] Alec Radford, Luke Metz, and Soumith Chintala. Unsupervised representation learning with deep convolutional generative adversarial networks. *arXiv preprint arXiv:1511.06434*, 2015. **1**
- [27] Mohammad Rastegari, Vicente Ordonez, Joseph Redmon, and Ali Farhadi. Xnor-net: Imagenet classification using binary convolutional neural networks. In *Proceedings of the European Conference on Computer Vision (ECCV)*, pages 525–542. Springer, 2016. **1**
- [28] Shaoqing Ren, Kaiming He, Ross Girshick, and Jian Sun. Faster r-cnn: Towards real-time object detection with region proposal networks. In *Proceedings of the Advances in Neural Information Processing Systems (NeurIPS)*, pages 91–99, 2015. **1**
- [29] Adriana Romero, Nicolas Ballas, Samira Ebrahimi Kahou, Antoine Chassang, Carlo Gatta, and Yoshua Bengio. Fitnets: Hints for thin deep nets. *arXiv preprint arXiv:1412.6550*, 2014. **1, 2, 4**
- [30] Olga Russakovsky, Jia Deng, Hao Su, Jonathan Krause, Sanjeev Satheesh, Sean Ma, Zhiheng Huang, Andrej Karpathy, Aditya Khosla, Michael Bernstein, et al. Imagenet large scale visual recognition challenge. *International Journal of Computer Vision (IJCV)*, 115(3):211–252, 2015. **2, 6**
- [31] Chengchao Shen, Xinchao Wang, Jie Song, Li Sun, and Mingli Song. Amalgamating knowledge towards comprehensive classification. In *Proceedings of the AAAI Conference on Artificial Intelligence (AAAI)*, pages 3068–3075, 2019. **4**
- [32] Guocong Song and Wei Chai. Collaborative learning for deep neural networks. In *Proceedings of the Advances in Neural Information Processing Systems (NeurIPS)*, pages 1832–1841, 2018. **1, 3, 4**
- [33] Christian Szegedy, Wei Liu, Yangqing Jia, Pierre Sermanet, Scott Reed, Dragomir Anguelov, Dumitru Erhan, Vincent Vanhoucke, and Andrew Rabinovich. Going deeper with convolutions. In *Proceedings of the IEEE Conference on Computer Vision and Pattern Recognition (CVPR)*, pages 1–9, 2015. **1, 6**
- [34] Yonglong Tian, Dilip Krishnan, and Phillip Isola. Contrastive representation distillation. *arXiv preprint arXiv:1910.10699*, 2019. **2**
- [35] Xiaojie Wang, Rui Zhang, Yu Sun, and Jianzhong Qi. Kdgan: Knowledge distillation with generative adversarial networks. In *Proceedings of the Advances in Neural Information Processing Systems (NeurIPS)*, pages 775–786, 2018. **2**
- [36] Guodong Xu, Ziwei Liu, Xiaoxiao Li, and Chen Change Loy. Knowledge distillation meets self-supervision. *arXiv preprint arXiv:2006.07114*, 2020. **2**
- [37] Ting-Bing Xu and Cheng-Lin Liu. Data-distortion guided self-distillation for deep neural networks. In *Proceedings of the AAAI Conference on Artificial Intelligence (AAAI)*, pages 5565–5572, 2019. **3**
- [38] Junho Yim, Donggyu Joo, Jihoon Bae, and Junmo Kim. A gift from knowledge distillation: Fast optimization, network minimization and transfer learning. In *Proceedings of the IEEE Conference on Computer Vision and Pattern Recognition (CVPR)*, pages 4133–4141, 2017. **2**
- [39] Li Yuan, Francis EH Tay, Guilin Li, Tao Wang, and Jiashi Feng. Revisiting knowledge distillation via label smoothing regularization. In *Proceedings of the IEEE Conference on Computer Vision and Pattern Recognition (CVPR)*, pages 3903–3911, 2020. **3**
- [40] Sergey Zagoruyko and Nikos Komodakis. Paying more attention to attention: Improving the performance of convolutional neural networks via attention transfer. *arXiv preprint arXiv:1612.03928*, 2016. **1, 2, 5, 7**
- [41] Sergey Zagoruyko and Nikos Komodakis. Wide residual networks. *arXiv preprint arXiv:1605.07146*, 2016. **6**
- [42] Linfeng Zhang, Jiebo Song, Anni Gao, Jingwei Chen, Chenglong Bao, and Kaisheng Ma. Be your own teacher: Improve the performance of convolutional neural networks via self distillation. In *Proceedings of the IEEE International Conference on Computer Vision (ICCV)*, pages 3713–3722, 2019. **3**
- [43] Xiaobing Zhang, Shijian Lu, Haigang Gong, Zhipeng Luo, and Ming Liu. Amln: Adversarial-based mutual learning network for online knowledge distillation. In *Proceedings of the European Conference on Computer Vision (ECCV)*, pages 158–173, 2020. **1, 7**
- [44] Xiangyu Zhang, Jianhua Zou, Xiang Ming, Kaiming He, and Jian Sun. Efficient and accurate approximations of nonlinear convolutional networks. In *Proceedings of the IEEE Confer-*

ence on Computer Vision and Pattern Recognition (CVPR), pages 1984–1992, 2015. [1](#)

- [45] Ying Zhang, Tao Xiang, Timothy M Hospedales, and Huchuan Lu. Deep mutual learning. In *Proceedings of the IEEE Conference on Computer Vision and Pattern Recognition (CVPR)*, pages 4320–4328, 2018. [1](#), [2](#), [3](#), [4](#), [7](#), [8](#)
- [46] Jun-Yan Zhu, Taesung Park, Phillip Isola, and Alexei A Efros. Unpaired image-to-image translation using cycle-consistent adversarial networks. In *Proceedings of the IEEE International Conference on Computer Vision (ICCV)*, pages 2223–2232, 2017. [1](#)
- [47] Xiatian Zhu, Shaogang Gong, et al. Knowledge distillation by on-the-fly native ensemble. In *Proceedings of the Advances in Neural Information Processing Systems (NeurIPS)*, pages 7517–7527, 2018. [1](#), [2](#), [3](#), [4](#), [7](#), [8](#)